NSLS-II BPM SYSTEM PROTECTION FROM ROGUE MODE COUPLING*

A. Blednykh#, B. Bacha, A. Borrelli, M. Ferreira, H.-C. Hseuh, C. Hetzel, B. Kosciuk, S. Krinsky, O. Singh, K. Vetter, BNL, Photon Sciences, Upton, New York, 11973-5000, U.S.A.

Abstract

Rogue mode RF shielding has been successfully designed and implemented into the production multipole vacuum chambers. In order to avoid systematic errors in the NSLS-II BPM system we introduced frequency shift of HOM's by using RF metal shielding located in the antechamber slot of each multipole vacuum chamber. To satisfy the pumping requirement the face of the shielding has been perforated with roughly 50 percent transparency. It stays clear of synchrotron radiation in each chamber.

INTRODUCTION

A new 3GeV NSLS-II storage ring is under construction at Brookhaven National Laboratory. The ring has a 30 cell double-bend achromatic (DBA) lattice [1]. Six beam position monitors (button type) per cell are going to be located on multipole vacuum chambers to measure and control electron beam trajectory. Each vacuum chamber in each cell is numerated in according to girder location. Five types of multipole vacuum chambers are going to be used in the NSLS-II storage ring [1], S2 Even, S2 Odd, S4, S6 Even and S6 Odd. They have the same cross-section profile and differ mostly in length.

The NSLS-II multipole vacuum chamber profile is shown in Figure 1. The full horizontal and vertical aperture of the beam channel is *76mm* x *25mm* respectively. The antechamber slot with a gap of 10mm is extended up to a trapezoidal area with a vertical aperture of 44mm. The NSLS-II BPM buttons are located on top and bottom of multipole vacuum chambers. There is a concern that existence of rogue modes observed in vacuum chambers with antechamber slot [2] can affect precision of the NSLS-II BPM diagnostic system. Rogue modes, which are classified as modes with Transverse Electric field (H-mode) in a ridged waveguide, can couple to the BPM buttons at frequencies near to the RF. It can produce a noise in BPM system and difficulties in monitoring of beam position in the ring.

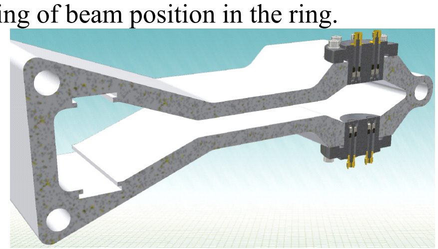

Figure 1: NSLS-II multipole vacuum chamber profile.

Since the NSLS-II multipole vacuum chamber profile has a complex geometry, the cutoff wavelength has been simulated numerically using the GdfidL code [3].

$$\lambda_c = 0.695m\,.$$

Since the cutoff wave length is known a set of resonance modes can be generated in a chamber at frequencies

$$f^H_{mnp} = \frac{c}{2\pi}\sqrt{\left(\frac{2\pi}{\lambda_c}\right)^2 + \left(\frac{p\pi}{L}\right)^2}\,,$$

where c is the velocity of light, λ_c is the cutoff wavelength, $p=1,2,\ldots k$ and L is the chamber length. Based on Maxwell's equations the first lowest mode like in a ridged cavity depends on the structure length (H_{101}-mode). Index p cannot be equal zero ($p \neq 0$). For a length of $L=3553mm$ (length of the S2-chamber), the first resonant frequency is f^H_{101} = *434MHz*. It agrees well with the frequency of the dominant mode obtained due to numerical simulations and microwave measurements (Table 1). Frequencies of the first six H_{mnp}-modes are shown in Table 1. The frequency of H_{106}-mode is almost equal to the RF frequency. In order to avoid interference of H-modes (TE-modes) with the BPM signal, the RF shielding is required.

Table 1: Frequency comparison of the H_{10p}-modes for the S2 multipole vacuum chamber with a length of 3553mm

Mode	Measurements f, MHz	GdfidL f, MHz	Equation f, MHz
H_{101}	430	434	434
H_{102}	436	440	440
H_{103}	446	450	450
H_{104}	458	463	464
H_{105}	478	480	481
H_{106}	496	500	501
H_{107}	518	523	523

BASIC CONCEPT OF ROGUE MODE SHIELDING

We have specified requirements for rogue mode shielding in reference 4 and 5. One way to avoid signal interference with frequencies of rogue modes is a wideband frequency shift by insertion of RF metal shielding into the chamber. Since the cutoff frequency f_c of the H_{10}-mode depends on geometric parameters such as a, a', b and b' the width of the chamber can be reduced by introducing the RF shielding at a distance D as shown in Fig. 2. It gives an opportunity to shift frequencies of H-modes above required frequency of 530 MHz.

*Work supported by DOE contract No: DE-AC02-98CH10886
#blednykh@bnl.gov

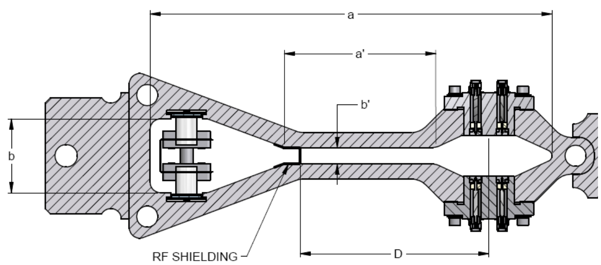

Figure 2: NSLS-II multipole vacuum chamber profile.

A simple RF shielding design was chosen with a cross section shaped such that it could be inserted into the aft section of the 10mm extraction slot adjacent to the anti-chamber (Fig. 3). This is an ideal location in part because in five out of six BPM locations, ray tracings revealed no radiation here that could damage the shield. Beryllium copper (BeCu) was chosen for it's high elastic modulus, giving the shield adequate spring force to retain it in the extraction slot. To satisfy the pumping requirement, it was necessary to perforate the face of the shield with roughly 50 percent transparency. This resulted in an array of 6.6mm square apertures spaced on 7.5mm intervals, small enough so the fields could not penetrate but large enough for adequate pumping. Notching the wings of the shield every 25mm allowed it to be produced using traditional progressive tool stamping technology which in turn allowed the shields to be produced in a continuous length then cut to the size needed for each chamber.

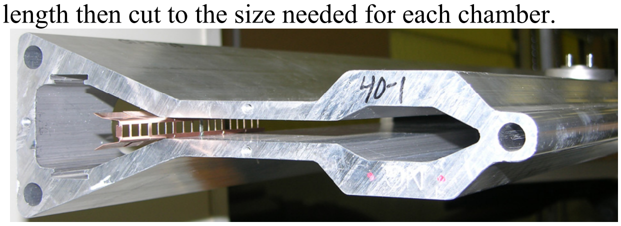

Figure 3: Flexible BeCu RF shielding with 50% of opening inside the multipole vacuum chamber. The thickness of the RF shielding is 0.25mm.

MICROWAVE MODE MEASUREMENTS IN PRODUCTION CHAMBERS

We have presented our measurements and comparison with numerical and analytical results for prototype chambers [5], since the production chambers were not available at that time. Here we present data for the production chambers S2, S4 and S6 which are being installed into the ring.

S4 Production Chamber

S4 production chamber has been loaded with flexible BeCu RF shielding at a distance D=114mm from the beam pipe center. Two separate RF shields of 2.2m and 460mm length are required in order to provide shielding before and after the stick absorber (Fig. 4). Since the stick absorber splits the chamber into two sections with different lengths we measured S21-parameter in each of the sections. In the long-length section the first resonant peak of H_{101}-mode is generated at frequency *973MHz*. In the short-length section the first lowest frequency of H_{101}-mode is *1GHz* (Fig. 5). Since the stick absorber is ungrounded and located close to the downstream BPM assembly, two locally generated resonances due to the stick absorber are observed at frequencies of 554MHz and 782MHz.

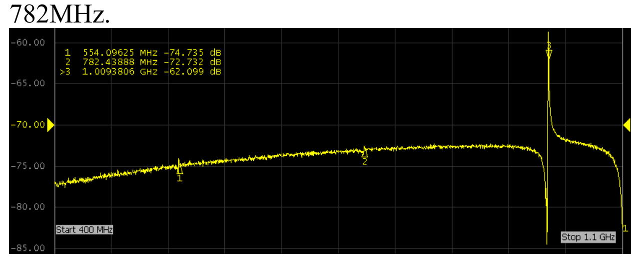

Figure 5: Measured S21-parameter in the S4 production chamber with RF shielding inside (logarithmic scale). Input and output signals are taken from downstream BPM.

S2-Vacuum Chamber

S2 even chamber has been measured in the same manner as S4 chamber. Since the stick absorber is located close to end of the chamber, only one RF shield with a length of ~3.5m has been loaded. The lowest frequency measured in the chamber is 965MHz (Fig. 6). The proposed shield works properly, effectively shifting the frequencies sufficiently higher than required.

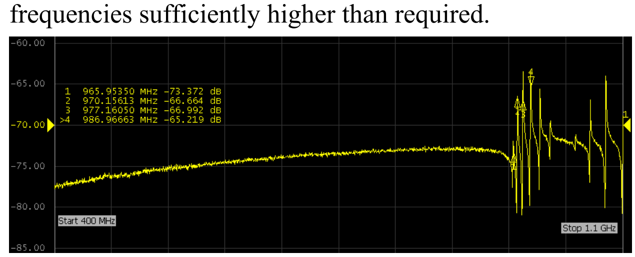

Figure 6: Measured S21-parameter in the S2 production chamber with RF shielding inside (logarithmic scale). Input and output signals are taken from upstream BPM.

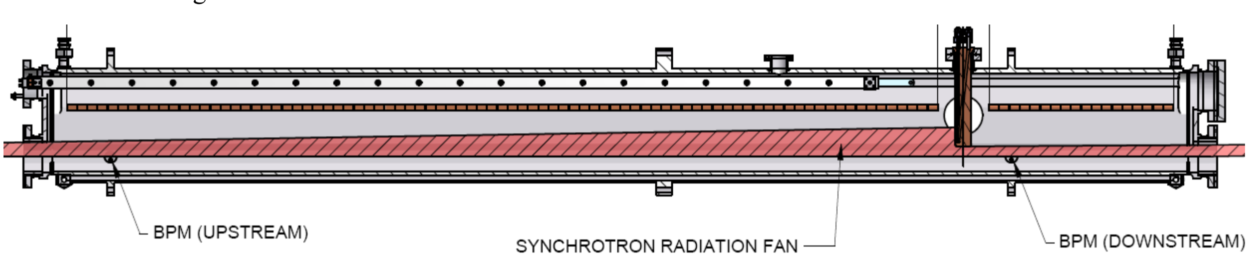

Figure 4: S4 chamber with RF shielding inside. The red shaded region represents the synchrotron radiation fan.

S6-Vacuum Chamber

The RF shielding length inside the S6 chambers, even and odd, has to stay clear of synchrotron radiation (red shaded color in Fig. 7) from downstream bending magnets. The emission angle in the horizontal direction at downstream of each S6 chamber is pretty large. The RF shielding has to end at a distance of ~2m away from the right side of the chamber (keeping the same horizontal distance of D=114mm) to avoid its heating and damage due to synchrotron radiation. The total inner length of the S6 even and odd chambers are 3559mm and 3445mm, respectively. This makes it difficult to protect the downstream BPM button in S6 chamber with ~2m of unshielded space.

We are considering the following possibility here. The length of the RF shielding is optimized so that 500 MHz frequency is centred between two neighbouring frequencies of H_{10p}-modes, which are generated in the empty space. In this case the frequency separation between two modes has to be more than $\Delta f = 20$ MHz to be outside the frequency range of the bandpass filter centred at 500 MHz [4]. With RF shielding length of 1346mm in S6 even and odd chambers (Figs. 8, 9) we are able to keep frequencies outside assigned range.

The RF shielding length has to be long enough too to protect the upstream BPM Button from rouge mode coupling.

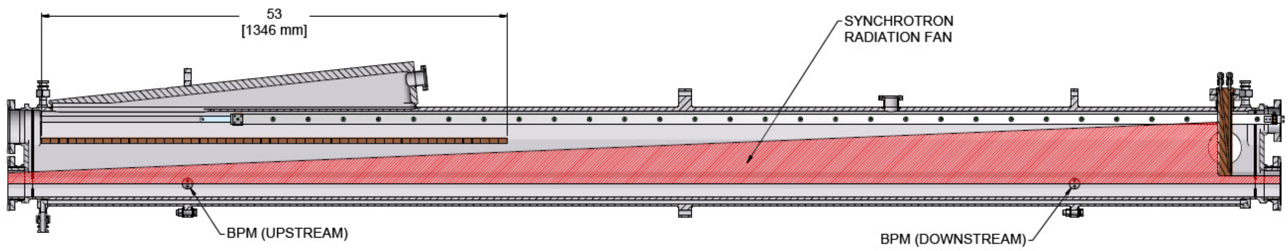

Figure 7: S6 even multipole vacuum chamber with RF shielding inside. The red shaded region represents the synchrotron radiation fan. Flexible BeCu RF shielding is 1346mm long.

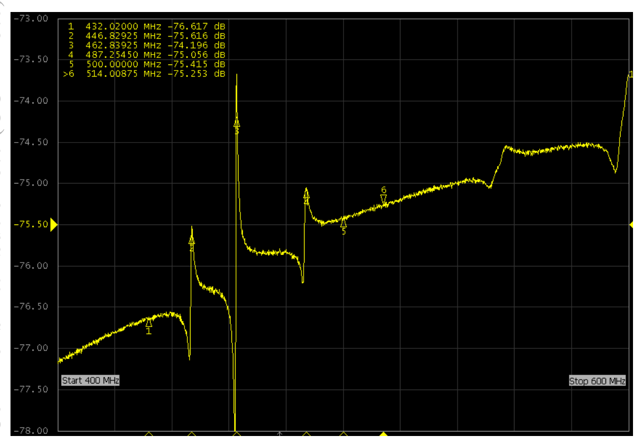

Figure 8: Measured S21-parameter in the S6 even production chamber (3559mm inner length) with RF shielding inside (logarithmic scale). Input and output signals are taken from downstream BPM.

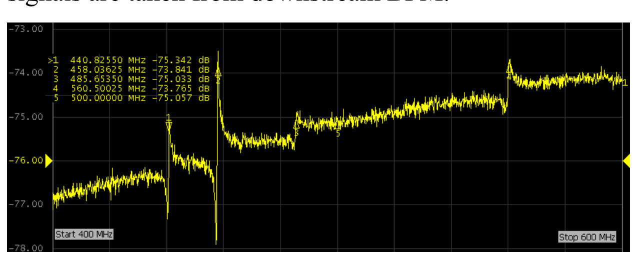

Figure 9: Measured S21-parameter in the S6 odd production chamber (3445mm inner length) with RF shielding inside (logarithmic scale). Input and output signals are taken from downstream BPM.

CONCLUSION

We demonstrated numerical modelling and experimental studies of the spurious TE modes in the NSLS-II vacuum chambers with antechamber slot. Calculated frequencies of TE-modes in considered chambers with and without RF shielding were verified experimentally. Flexible BeCu RF shielding inside each chamber at proper location shifts frequencies of H_{10p}-modes above required frequency of 530MHz except chambers S6 odd and even. In S6 chambers we have optimized the RF shielding length to keep each downstream BPM Button clear of rogue mode coupling at frequencies near to the RF.

RF shielding looks adequate for baseline design. Fifty percent of open space provides adequate pumping speed.

REFERENCES

[1] NSLS-II Preliminary Design Report, 2008; http://www.bnl.gov/nsls2/project/PDR/
[2] Y. Kang, G. Decker and J. Song, "Damping spurious harmonic resonances in the APS storage ring beam chamber," EPAC'96, Sitges, June 1996, p. 7984 (1997).
[3] W. Bruns, GdfidL code; http://www.gdfidl.de
[4] K. Vetter et al., "NSLS-II RF Beam Position Monitor", BIW10, Santa Fe, NM, US.
[5] A. Blednykh et al., "Rogue Mode Shielding in NSLS-II Multipole Vacuum Chambers", Proceedings of BIW10, Santa Fe, New Mexico, US. P194 (2010).